Computer Science Department Technical Report
University of California
Los Angeles, CA 90024-1596

EXCITATION WAVE PROPAGATION WITHIN NARROW PATHWAYS: GEOMETRIC CONFIGURATIONS FACILITATING UNIDIRECTIONAL BLOCK AND REENTRY

B. Kogan
W. Karplus
B. Billett
W. Stevenson

November 1991
CSD-910078

Excitation Wave Propagation Within Narrow Pathways: Geometric Configurations Facilitating Unidirectional Block and Reentry

Boris Y. Kogan[1] Walter J. Karplus, Brian S. Billett
Computer Science Department, UCLA
William G. Stevenson
Department of Cardiology, UCLA

[1]Address for correspondence: Boris Y. Kogan, PhD, Computer Science Department, UCLA, 3732 Boelter Hall, 405 Hilgard Ave., Los Angeles, CA 90024, telephone (213)825 7393, fax (213)825 2273, e-mail kogan@cs.ucla.edu.

Research in the use of massive parallelism for system simulation in the UCLA Computer Science Department is supported in part by the NASA/Dryden Research Center under Grant NCC 2-374 and NSF Grant BBS 87-14206.

Running title: Wave Propagation Within Narrow Pathways.

Key words: myocardial infarction, reentry, wave propagation, computer simulation, ventricular tachycardia, sudden death.

Abstract

Reentrant arrhythmias are common in the presence of myocardial infarct scars where regions of normal tissue are interspersed with inexcitable ones. We hypothesize that variations in geometry of the surviving myocyte pathways in areas of chronic infarction may cause unidirectional block and reentry. To determine the role of pathway geometry a theoretical study and computer simulations are performed. Two idealized geometric configurations are considered: propagation through narrow paths with either parallel or tapered borders. Border tissue either allowed zero current flux or served as a current sink. Using the relationship between stationary speed of wave front propagation and its curvature, it is shown that unidirectional block can occur in narrow paths with parallel borders and "zero flux" boundary conditions where the wave leaves the narrow path and emerges into an open area of appropriate size. In narrow paths with parallel borders and border tissue serving as a current sink, propagation is either "all" or "none", and unidirectional block is impossible. The wave blocked or propagated in both directions depending on its pathway width. Unidirectional block can occur, however, when the narrow path has a tapered shape. Waves propagating from the wide end of the pathway die out at the narrow end, while waves propagating in the opposite direction are able to pass through. In computer simulations of a two dimensional grid of 128x128 membrane segments using the modified FitzHugh-Nagumo equations, the arrangement of two or more pathways in parallel permits reentry if at least one pathway has a configuration causing unidirectional block, and the cells at the site of unidirectional block have sufficient time to recover from the previous excitation. The latter is facilitated by anisotropic conduction properties tissue especially in cases of "zero flux" border conditions. Thus, specific geometric configurations of narrow pathways exist which allow reentry even when membrane properties and intercellular resistance are uniform.

INTRODUCTION

Reentry circuits causing ventricular tachycardia late after myocardial infarction often involve strands of surviving ventricular myocyte bundles which form narrow paths for impulse propagation through areas of infarct scar (deBakker et.al.[1], Bolick et.al.[2], Fenoglio et.al.[3], deBakker et.al.[4]). These strands vary in both width and length, and strands may branch or coalesce forming complex patterns. Despite evidence of depressed conduction throughout the infarct scar, the surviving myocytes often have normal action potentials (deBakker et.al.[1], Spear et.al.[5], Gardner et.al.[6], Denniss et.al.[7]), and increased intercellular resistance may promote unidirectional conduction block and slow propagation, which facilitate reentry (Dillon et.al.[8], Spear et.al.[5], Ursell et.al.[9], Gardner et.al.[6]). The role of the myocyte bundle geometrical arrangement and dimensions in slowing conduction and in unidirectional block is not clear. Studies of propagation between blocks of atrial tissue connected by a narrow isthmus (de la Fuentes [10], Inoue and Zipes [11]) and across Purkinje fiber-muscle junctions (Mendez [12]) have shown that unidirectional block tends to occur where an excitation wavefront propagates from a narrow path of tissue to a larger mass of excitable tissue. Impulse propagation over an isthmus of atrial tissue was inversely related to the cross sectional area of the isthmus (Inoue and Zipes [11]). This behavior is consistent with "impedance mismatch" such that the current generated from the narrow path is insufficient to bring a larger mass of tissue to threshold.

The present investigation was undertaken to determine the relation of pathway geometry to wavefront propagation. Studies of wave propagation through different excitable media have previously shown that the conduction velocity is dependent on the curvature of the stationary propagating wavefront (Zykov [13], Tyson [14]). The propagation velocity decreases as the absolute value of negative wave front curvature increases. In addition, a critical value of wave front curvature and a corresponding critical speed of propagation exist, beyond which propagation becomes impossible. These general properties apply for any type of mathematical model or real excitable tissue, differing only quantitatively for each specific model, and are valid for isotropic as well as for anisotropic tissue. (see Kogan et.al.[15]) In this study, we apply the concept of wave front curvature in relation to the geometry of narrow pathways for propagation and also investigate the effect of border tissue properties. Effects of pathway shape, size relative to surrounding excitable tissue, electrical properties of border zones, action potential duration (APD) restitution and anisotropy were considered for theoretical study and computer simulations of a two dimensional sheet of excitable elements.

Idealized corridors of uniformly excitable normal tissue (isotropic and anisotropic) were considered in these studies. The effect of pathway geometry on conduction velocity was shown to be related to the accompanying effects on the curvature of the propagating wavefront, consistent with previous studies of wave front propagation in excitable media (Zykov [13], Tyson [14]). Specific geometric configurations cause unidirectional conduction failure, slow conduction velocity and produce reentry in two dimensional sheets of excitable elements, even when the electrical properties of each element are identical. For some cases these effects are more pronounced in the presence of anisotropic conduction (Wit[16]). This suggests that for certain geometric configurations of surviving muscle bundle strands in chronic myocardial infarction alteration of active membrane properties or an increase in intercellular resistance within the conduction pathways may not be required for reentry.

METHODS AND MATERIALS

Theoretical Studies

We assume that the dimensions of these narrow paths are considerably larger than those of the cell. This allows us to limit the study to macroprocesses. The results of microprocesses are described in Spach[17], and Rudy and Quan[18]. Propagation through excitable isthmuses were considered for pathways of two basic configurations: 1. pathways with regular, parallel borders of various widths, and 2. funnel shaped pathways.

The characteristics of the areas bordering surviving myocyte bundles in areas of a scar have not been established. Therefore three possible situations were considered. First, the current between the isthmus and border zone tissue may be zero as if the coupling resistance between these regions is infinite, as may occur with connective tissue. We call this the "zero flux" border condition. Second, the border zone may act as an abnormal current sink. This could occur if the border areas consisted of an electrolyte solution, which decreases the coupling resistance between the isthmus and the border tissue; or the border tissue contained surviving myocytes with markedly depressed excitability, or which had markedly prolonged recovery times. Myocytes with the latter characteristics have been observed to coexist in the same infarct as myocytes with relatively normal membrane characteristics (deBakker[1], Gilmour[19], Spear[5], Myerburg[20]). The extent to which myocytes with depressed excitability can serve as an current sink serves a basis for dividing border tissues into two groups: 1. "moderate current sink", or 2. in a "limit case", border tissue which acts as a "large" current sink.

Propagation through normal ventricular tissue is anisotropic, due to greater intercellular resistance

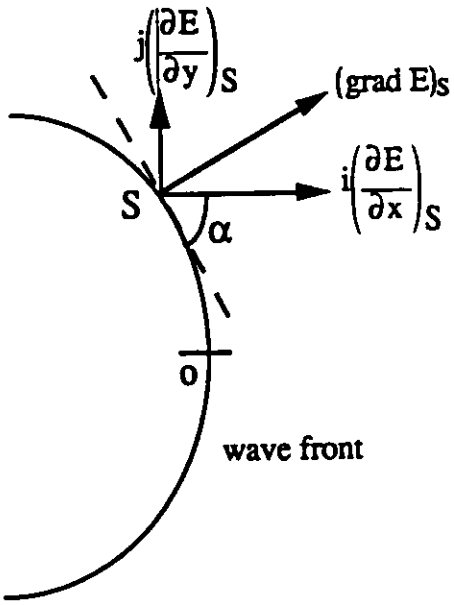

FIG. 1. Wave front shape and the components of grad$E$.

in the transverse axis of myocytes as compared to the longitudinal axis. In infarct scars anisotropic conduction is maintained and can be accentuated (Dillon[8]). Anisotropy is modeled by appropriately altering resistance between excitable elements. The shape of the wave front can be defined as a function $\alpha = f(s)$, where α is the angle of the tangent of the front of the wave at a point "s" taken on the chosen equipotential $E = const$. This angle is measured with respect to the Cartesian coordinate x (see Fig. 1) and can be expressed in terms of the components of grad$E$ in the direction of current flow, which is normal to the front of the wave at all points. Therefore $\tan\alpha = \frac{\partial E}{\partial x}/\frac{\partial E}{\partial y}$. We now apply these considerations to estimate the form of the wave front and its curvature inside the narrow paths.

For the tissue with parallel borders of zero flux type, the component of grad$E$ along the y axis $\partial E/\partial y = 0$ at all points on the border, and the angle of the tangent to the wave front at all points of the border must be $\pi/2$. The wave front is rectilinear (see Fig. 2 a) with a curvature $K = 0$.

For the case when the borders of narrow paths serve as a large current sink, it is possible to assume that the border cells are held at rest potential, so that the grad$E$ component $\partial E/\partial x$ is equal zero at all points of the border, and the angle α equals zero at that points. Inside the narrow path this component of grad$E$ and the angle α increase until they reach maximum values: $gradE = (gradE)_{max}$ and $\alpha = \pi/2$ at the midpoint of wave front. It is therefore reasonable to approximate the wave front inside a narrow path as a semi-circle with a radius equal to $W/2$ and a curvature $K = 2/W$.

When the border tissue serves as a moderate current sink, the angle of the tangent at the border

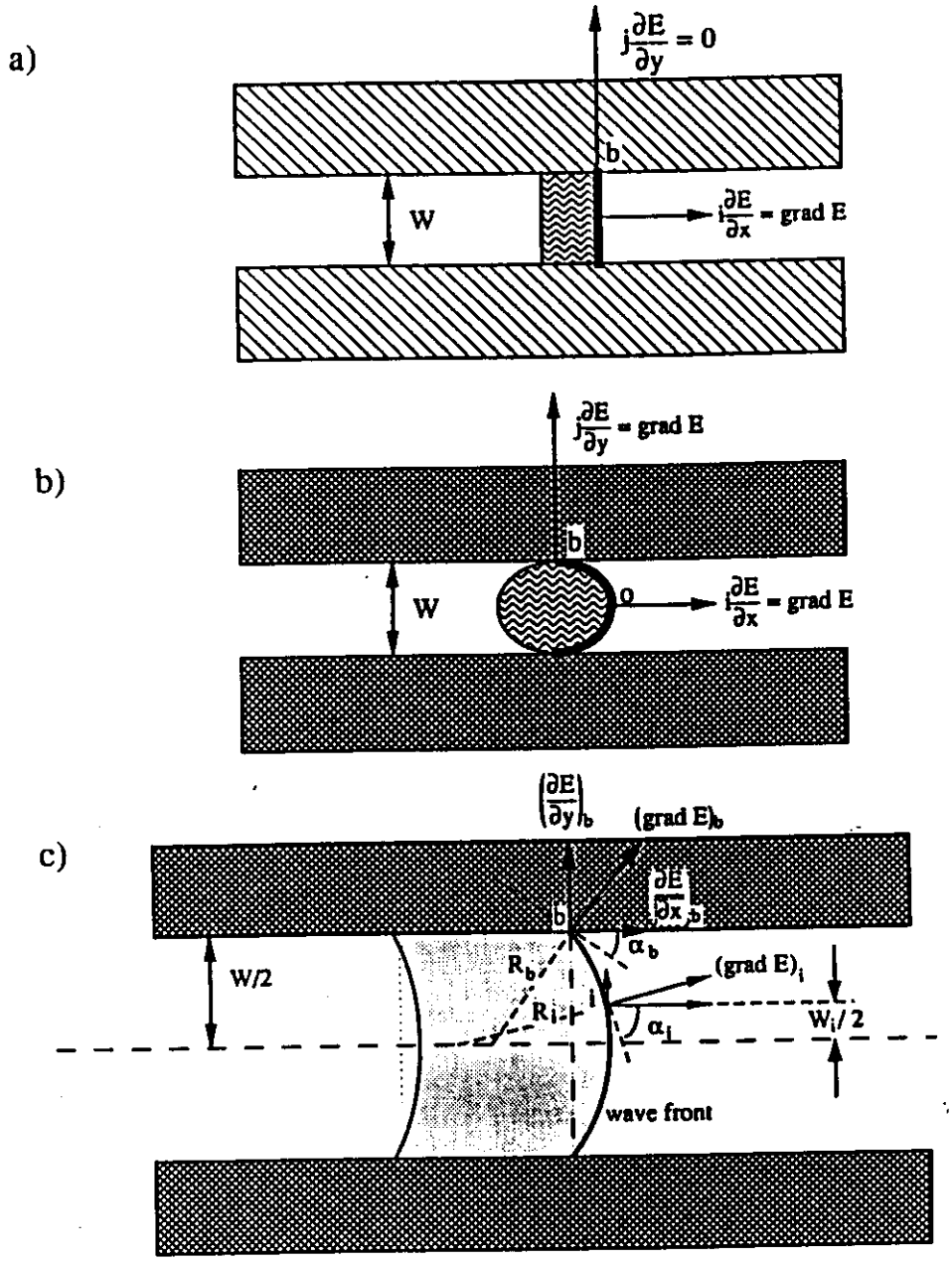

FIG. 2. Shapes of wave fronts inside narrow paths with border tissue of different properties. "W" – channel width; "b" – point of intersection of border with wave front; "0" – mid point of wave front; "i" – point on wave front; R_i, R_b – radii of wave front; α_i, α_b – angles to tangent on wave front. a. Rectilinear wave front inside a narrow path with border tissue of "zero flux" type, K = 0. b. Semicircular wavefront inside a narrow path with "large current sink" border tissue, K = W/2. c. Wave front inside narrow path with "moderate current sink" border tissue, $K_i = \cos\alpha/((W_n/2)+(L-L_i)\tan\beta)$.

points is determined by the ratio of the corresponding components of grad$E$. Because the path is narrow, we can approximate the wave front as a part of a circle with radius $R_b = W/(2\cos\alpha_b)$ and curvature $K_b = 1/R_b$

$$K_b = \frac{2}{W}\cos\alpha_b = \frac{2}{W}\frac{1}{\sqrt{1+\tan^2\alpha_b}} \tag{1}$$

where:

$$\tan\alpha_b = (\frac{\partial E}{\partial x})_b/(\frac{\partial E}{\partial y})_b \tag{2}$$

Similarly, for any point "i" in Fig. 2 except point "0" on the wave front the curvature is found to be:

$$K_i = \frac{2}{W_i}\cos\alpha_i = \frac{2}{W_i}\frac{1}{\sqrt{1+\tan^2\alpha_i}} \tag{3}$$

where:

$$\tan\alpha_i = (\frac{\partial E}{\partial x})_i/(\frac{\partial E}{\partial y})_i \tag{4}$$

Fig. 2 a,b,c. show all the geometric constructions which were used to derive these formulas. The grad$E$ components necessary to determine the angle α_i at the chosen point on the wave front, can be obtained during the computer simulation for a particular tissue model.

Computer Simulations

The theoretical considerations do not depend on the properties of a particular model; its results have a generalized significance and show, as a rule, the qualitative characteristics of wave propagation processes in the context of the assumptions. Computer simulations are used to obtain the quantitative characteristics for the FitzHugh-Nagumo model, to verify that the assumptions of the theoretical study are valid for this model, and to determine how the effects of geometry, border tissue conditions, anisotropy, and APD restitution, promote or inhibit reentry. To allow for potential reentry, two parallel paths for propagation connecting the larger regions of excitable tissue are simulated.

The basic model of 2-dimensional action potential propagation used in this study and its implementation on a massively parallel computer system, the Connection Machine - 2 (CM) has been previously described in Kogan et.al.[21]. The simulated rectangular tissue section consists of electrically connected 128x128 membrane segments defined by the simplified ventricular membrane model of the modified FitzHugh-Nagumo (F-N) equations, which includes the APD restitution properties (Kogan et.al.[22]). As detailed in [22], the APD restitution properties can be varied by changing

the value of the ε_4 parameter from 0.5 ($= \varepsilon_3$), which corresponds to rapid decay of the residual outward current or rapid APD restitution, to $\varepsilon_4 \leq \varepsilon_2$, which corresponds to slow decay of residual outward current and therefore slow APD restitution. The parameters of the dimensionless F-N equations used are: $G_f = 0.7$, $G_r = 30.0$, $G_s = 1.0$, $\varepsilon_1 = 0.5$, $\varepsilon_2 = 0.02$, $\varepsilon_3 = 0.5$, $\varepsilon_4 = 0.018$ (Kogan et.al[22]). Identical membrane properties were assigned to all segments unless otherwise noted. The F-N equations were solved numerically by the modified method of lines (Petrov[23]). Each CM processor solved the ordinary differential equation describing the dynamics of a single membrane segment (grid point) by the Runge-Kutta-2 method. Continuous diffusion in the 2-D model (Laplacian operator) was replaced by its finite difference approximation. The exchange of data from adjacent grid points for this calculation is performed after 2 integration steps. Integration step size and grid spacing correspond to 0.025 time units and 0.6 space units. For membrane capacitance $C = 4\mu F/cm^2$ 1 time unit = 2 msec., 1 space unit = 0.04 cm. A total simulation time (typical) of 2000 time units (4000 ms) required approximately 360 sec of real computation time.

Although the F-N model is an oversimplification of a real cardiac membrane segment, it has several important advantages: 1. The modified F-N model allows incorporation of action potential duration restitution properties. 2. The F-N model correctly reflects qualitative peculiarities of wave propagation. 3. The simplicity of the F-N model allows simulations on large grids of membrane segments. 4. Results from F-N simulations can be used to determine whether the theoretical assumptions are valid for the FN model.

Implementation on the Connection Machine has several important benefits. Since the CM is a massively parallel machine with SIMD architecture, its fast numerical solution allows interactive simulations, where parameters, stimuli, and tissue configuration can be altered at any time during a simulation. By instantaneously displaying the computed action potential and generalized outward current (see Kogan et.al.[22]), the relationship of outward current to action potential duration restitution, impulse propagation, and reentry can be visualized. Various colors in the graphics display correspond to action potential E and outward current I levels – here shown copied in black and white – see Fig. 3.

Variations in pathway geometry and border conditions were explored and tested against theoretical results. A region of "zero flux" border tissue were held at the same E level as neighboring pathway cells. Regions of moderate current sink border tissue were simulated by a set of grid points with $G_f <$ normal G_f. G_f is a parameter of the F-N model which determines the excitability of a cell and correspondingly its threshold level. In our implementation, a standard G_f value of 0.7 was

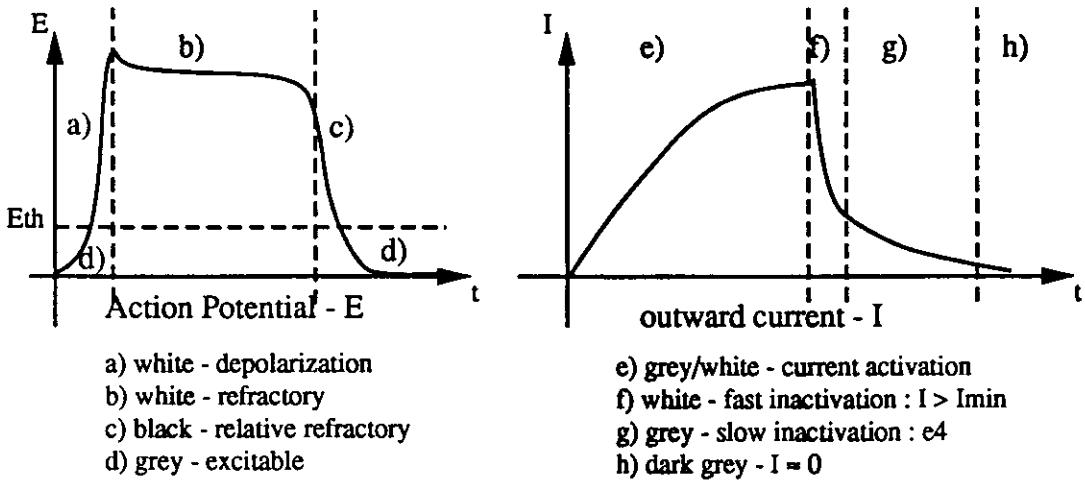

FIG. 3. Schematic representation of grey level designations for action potential E and current I phases.

chosen for viable tissue, and values of 0.1-0.5 were assigned to abnormal current sink tissue. Uniform anisotropic tissue was modeled by changing the diffusion coefficient ratio of x to y directions for all simulated membrane segments. In anisotropic tissue, diffusion in the x direction was generally 2 to 10 times greater than in the y direction. The finite difference approximation was computed with this ratio to simulate anisotropy. The initial stimulus was applied to a long rectangular region along one border, 128x4 cells. These nodes were held at a super-threshold current level ($I = 4.0$) for 4 time units, then the wave front propagated across the simulation field.

RESULTS

Wave Propagation and Unidirectional Block

Narrow pathways with "zero flux" borders—

The geometric configurations modeled are shown schematically in Fig. 4. By changing the value of the angle β from zero to $\pi/2$, it is possible to create a continuous transition from a narrow path with parallel borders to one with tapered borders with expanding openings. The limit when $\beta = \pi/2$ corresponds to the abrupt opening of the narrow path to the unrestricted right half-plane of the excitable tissue. Theoretical studies and computer simulations show that with the FN model in this type of channel with parallel borders, stationary waves propagate with a rectilinear front. The

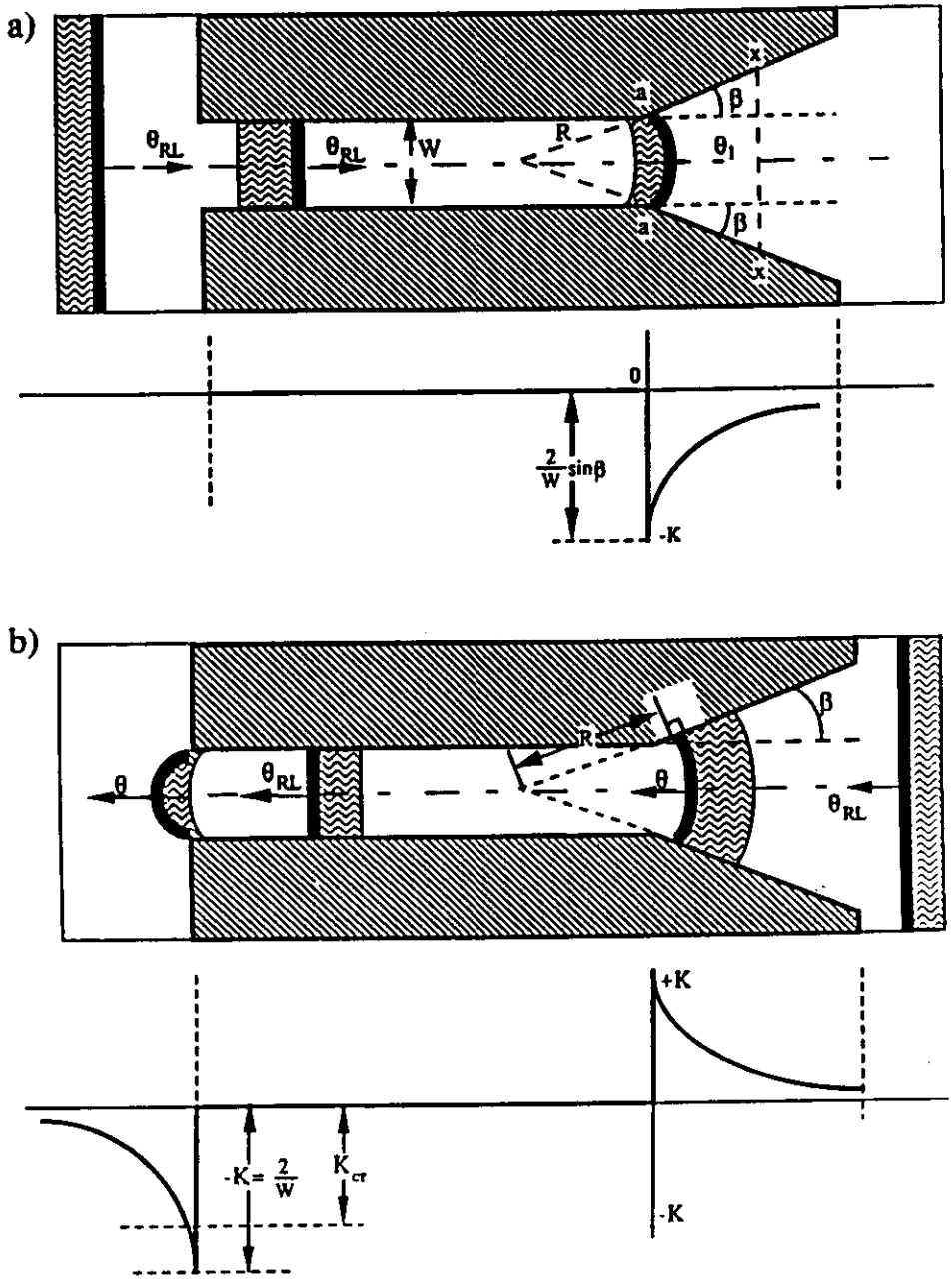

FIG. 4. Wave propagation in narrow pathways with border tissue of the "zero flux" type. Below each tissue configuration schematic, the wave front curvature values at all corresponding points (in the x direction) are shown. a. The wave passes when a rectilinear stimulus is applied at the left side of a narrow pathway; b. The wave dies out when the stimulus is applied at the right side of a narrow pathway.

wave front velocity is unchanged regardless of the channel width. Since the propagated wave front must be perpendicular to the borders at all points (see also the section *Methods and Materials - Theoretical Studies*), the wave front at the points "a-a" of the expanding borders can be considered, as a first approximation, to be an arc of a circle. The simple geometric drawing, shown on Fig. 4 a, gives:

$$R = W/(2\sin\beta) \tag{5}$$

or:

$$K = 1/R = (2\sin\beta)/W \tag{6}$$

Here:

R - radius of wave front at the pathway opening;

W - width of the pathway with parallel borders;

β - angle of border inclination;

K - curvature of the wave front at the points "a-a"

Equation (6) specifies a family of sinusoidal curves of amplitude $A = 2/W$ and is correct for all points "x-x" on the border of a tapered opening. It is necessary only to substitute in eqn. (6) the value of $W/2$ by its value $W_{x-x}/2$ at the points "x-x" (see Fig. 4 a). Geometry of this figure gives:

$$W_{x-x}/2 = (W/2) + (L - L_x)\tan\beta \tag{7}$$

Here:

L - full length of tapered part of pathway

L_x - distance from the wide end to points "x-x" of the tapered part

So, the curvature K_x will be:

$$K_x = \pm\frac{\sin\beta}{(W/2) + (L - L_x)\tan\beta} \tag{8}$$

The signs + and − correspond to concave and convex shapes of propagated wave fronts, respectively.

As discussed above, there exists a critical value of wave front curvature above which propagation becomes impossible, i.e there is a propagation block. Physically this means that the excited cells

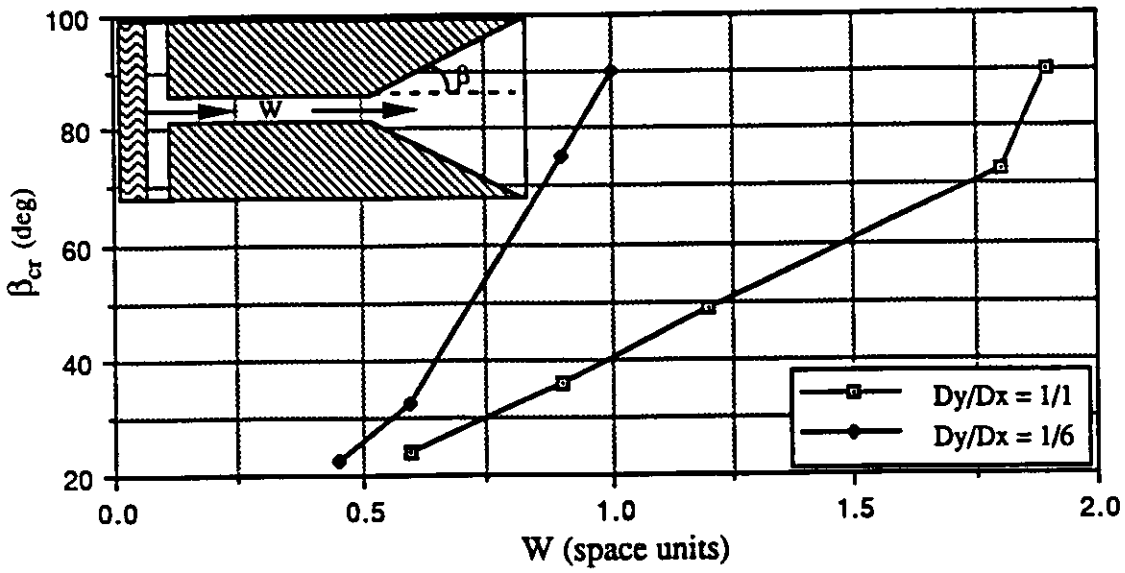

FIG. 5. Critical angle β for block at exit from narrow pathways with "zero flux" borders for various widths of pathways in isotropic and anisotropic tissue.

(sources) do not transmit enough electrical current to the neighboring non-excited cells (sinks) for them to reach the excitation threshold value. This critical value depends on the type of the selected membrane segment model and its parameter values. Let us assume that the value of K_{cr} is known. Then from equation (6) we obtain:

$$K_{cr} = \frac{2}{W} \sin \beta \tag{9}$$

and:

$$\beta = \arcsin \frac{K_{cr} W}{2} \tag{10}$$

Eqn. (7) and (8) give the relation of β_{cr} to W. Figure 5 shows the results of computer simulations used to determine this dependency for the FN model with isotropic and anisotropic tissue. The results for isotropic tissue differ somewhat from the predicted arcsin function due to the discrete nature of the simulation model. For the same β_{cr} value, the minimum channel width which allows propagation is smaller for anisotropic tissue (see Fig. 5). Figure 6 shows the same phenomena for a wide range of anisotropy ratios. This phenomenon can be explained by the decreased current consumption of neighboring segments of cells, located in the transverse direction when tissue anisotropy is increased.

The direct measurement of critical wave curvature is very difficult in physiological experiments. Computer simulations to determine the critical curvature require a comparatively large amount of calculations which grows with the complexity of the model. Eqn. (6) permits us to measure the

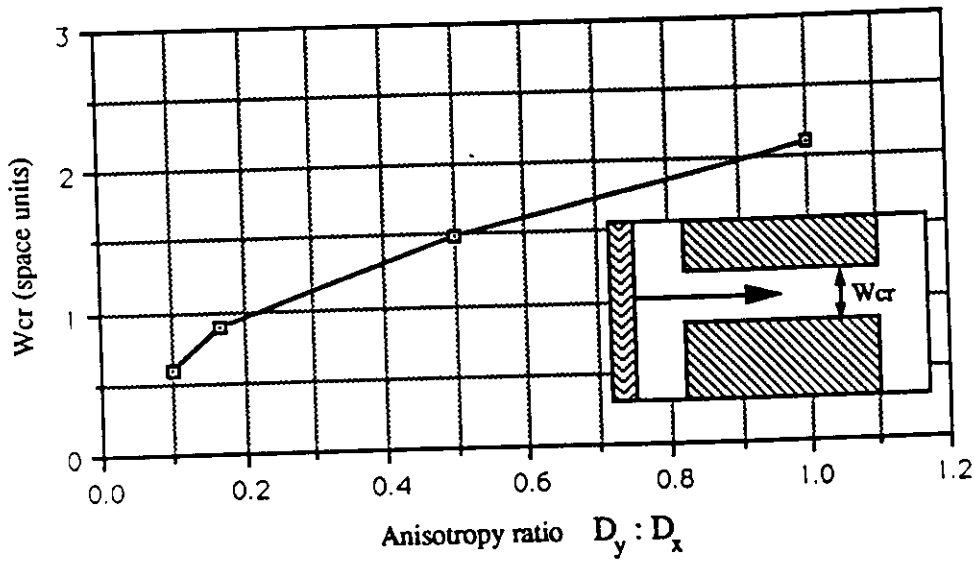

FIG. 6. Relationship of critical width (β is held constant at 90 deg) to anisotropy ratio, when propagation block in narrow paths with "zero flux" borders occurs.

width of the narrow pathway instead of the wave front curvature in order to obtain the critical value of wave front curvature. Indeed, for $\beta = \pi/2, K = 2/W$. By changing the width of the narrow pathway during computer simulation, one can find the $W = W_{cr}$ at which propagation through the opening becomes impossible.

The values for K_{cr} obtained by Zykov[13] for the FN model, using an approximate formula and repeated solution of the original equation ($K_{cr} = -0.79$), and that using our approach ($K_{cr} = -0.83$) are in close agreement.

Let us consider the configuration shown on Fig.4 a, where W is chosen so that $W = W_{cr}$ and $\beta = \pi/2$ (left entrance to the narrow path). When the wave propagates from left to right, its curvature remains equal to zero throughout the narrow path until it reaches the flared opening. Here the wavefront curvature abruptly changes from $K = 0$ to $K = K_{cr} \sin\beta$, and the wave propagates out of the narrow path without block. When the excitation wave is initiated from the right side of Fig. 4 b, it takes on a concave form in the tapered pathway, and where the borders of the narrow path become parallel, the curvature changes from a positive value to zero. At the left opening with $\beta = \pi/2$, the curvature abruptly changes from $K = 0$ to $K = K_{cr}$, and block of propagation occurs. When both ends of the narrow channel have an opening with $\beta = \pi/2$, wave fronts can enter the narrow path from either direction, but block at the opposite end of the path. Thus, only bidirectional block or propagation will occur, depending on the width of the channel. When the pathway is tapered over its entire length, the wave propagating from the wider end toward

the narrow end changes its curvature inside the channel from some positive value (see eqn (8)) to $K = -W/2$ at the narrow end. When $-W/2 = K_{cr}$, conduction block occurs. When the wave propagates in the opposite direction, the curvature of the wave front never exceeds the critical value. Hence unidirectional block is possible solely due to the spatial configuration of the pathway.

When the excitable tissue in Fig. 4 has anisotropic properties such that the resistance between elements is lower in the direction parallel to the long axis of the narrow pathway ($D_x/D_y > 1$), and hence conduction is more rapid in this direction, the creation of a unidirectional block is more difficult than with isotropic conduction. The component of the gradient ($\partial E/\partial y$) in anisotropic tissue is smaller than for isotropic tissue and, the wave front curvature is smaller when it exits a narrow pathway.

Narrow pathways with "current sink" borders—

It was shown earlier that the front of the wave inside a narrow path with "large current sink" type parallel borders can be estimated as a semicircle of radius $R = W/2$ and curvature $K = 2/W$. If the width (W) of the narrow path is greater than the critical width (W_{cr}), propagation can occur in either direction. If $W \leq W_{cr}$, waves from either direction die out inside the channel. Therefore, in uniform narrow pathways with large sink type parallel border tissue, unidirectional block does not occur.

Unidirectional block can occur, however, when the narrow path has the proper tapered shape. Waves propagated from the wide end of the tapered channel die out at the narrow end while waves propagated in the opposite direction are able to pass through. [1]

In order to explain this phenomenon, let us consider the geometry of the wave front inside the tapered channel at points "i-i" and at the narrow end (Fig. 7 a). When the borders tissue has the property of a large sink, the vector grad$E$ is everywhere perpendicular to the border lines at all of its points. The border lines serve in this case as a tangent to the wave front. Assuming as before, that the wave front inside the narrow tapered channel can be approximated by part of the circle, we obtain the expression for wave front curvature:

$$K_i = \frac{1}{(W_n/2) + (L - L_i)\tan\beta}\cos\beta \tag{11}$$

At the narrow exit from the path $L = L_i$, and we obtain:

[1] This phenomenon was observed in the course of computer simulation by A. Pang and B. Billett see Pang[24].

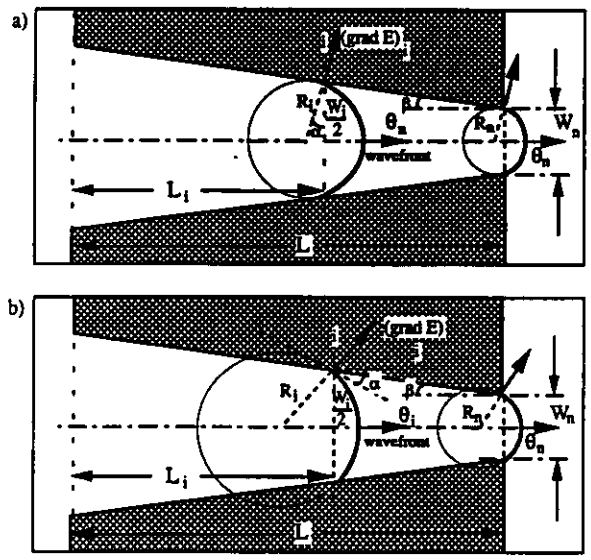

FIG. 7. Geometry for the determination of the curvature of wave fronts inside the tapered pathways. a) With borders of "large current sink" tissue. b) With borders of: "moderate current sink" tissue.

$$K_n = \frac{2}{W_n}\cos\beta \tag{12}$$

Observe that $K_n > K_i$. So, the site at which conduction block is most likely to occur is the narrow end of the tapered channel. If we neglect the transient processes of wave front curvature establishment associated with abrupt changes in pathway geometry, we can assert that the curvatures of the wave fronts crossing the narrow end in either direction are the same. Any directional differences are then due to differences in the length of the wave front arc relative to the size of the tissue into which the propagated wave must penetrate. The concept of source and sink leads to the conclusion that the wave propagated from the wide end to the narrow end of the tapered channel is more likely to be blocked than the wave propagated in the opposite direction.

The same reasoning can be applied to the case of border tissue serving as a moderate current sink. Unidirectional block is possible only in a tapered pathway of properly chosen geometry. The expression for the curvature at any border points "i" inside the channel (Fig. 7 b) can be obtained by replacing $\cos\beta$ in eqn. (9) by $\cos\alpha$:

$$K_i = \frac{1}{(W_n/2) + (L - L_i)\tan\beta}\cos\alpha = \frac{1}{(W_n/2) + (L - L_i)\tan\beta}\frac{1}{\sqrt{1 + tan^2\alpha_i}} \tag{13}$$

where:

$$\tan\alpha_i = (\frac{\partial E}{\partial x})_i/(\frac{\partial E}{\partial y})_i \tag{14}$$

At the narrow end $L = L_i$ and curvature $K = K_n$:

$$K_n = \frac{2}{W_n}\cos\alpha \tag{15}$$

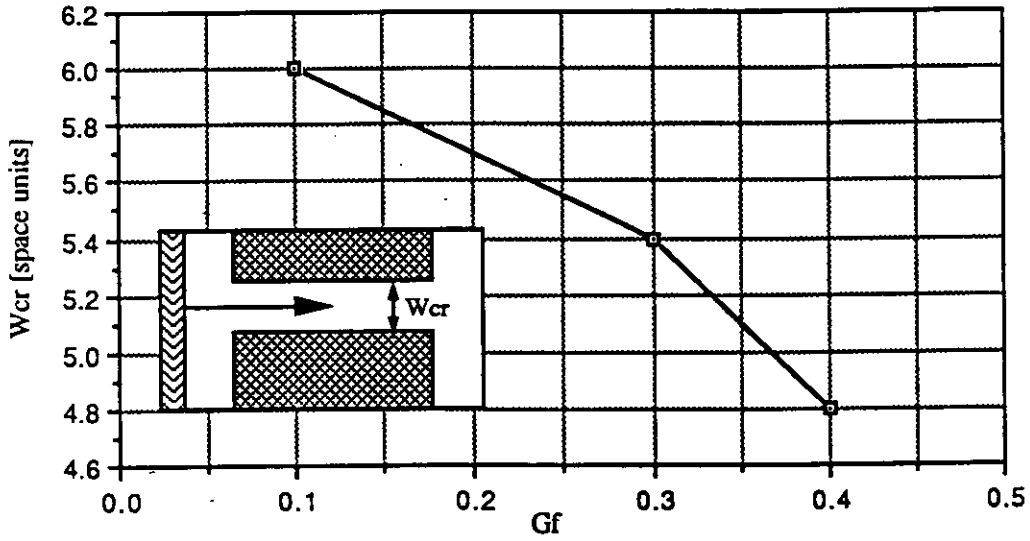

FIG. 8. Relationship of critical width, W_{cr}, for propagation block to the excitability (G_f) of the narrow pathway borders. As G_f increases, the border tissue current consumption decreases. Pathway borders are parallel.

Note that the waves propagated in both directions have the same curvature. As in the previous case, the wave front propagated toward the wide end has a larger arc and enters a smaller area of tissue than waves propagated in the opposite direction. In this case, unidirectional block can occur when the wave propagates from the wide end toward the narrow end of a tapered pathway.

It follows that geometric asymmetry is necessary for unidirectional block in narrow pathways when membrane properties are the same for either direction.

As in "zero flux" channels, certain pathways with borders serving as moderate current sinks will cause propagation block when exiting to a larger area of viable tissue. Fig. 8 shows computer simulation results for the determination of the critical width W_{cr} for various levels of current sink (G_f) for the pathway borders.

Computer simulations using the FN model reveal that for "current sink" bordered channels, it is possible to find combinations of the model parameters and tapered pathway geometric characteristics (G_f, β, and W_n) for which unidirectional block occurs. In Fig. 9, the simulation results for $G_f = 0.4$ are shown. Regions (parameter combinations) of bidirectional propagation, unidirectional block, and bidirectional block are labeled. The unidirectional block region's width increases with β, since for very small angles the wave has difficulty propagating into the channel. If the angle β is too large, however, waves can propagate through the channel in both directions. As the current sink increases (smaller G_f), the larger W_{cr} becomes.

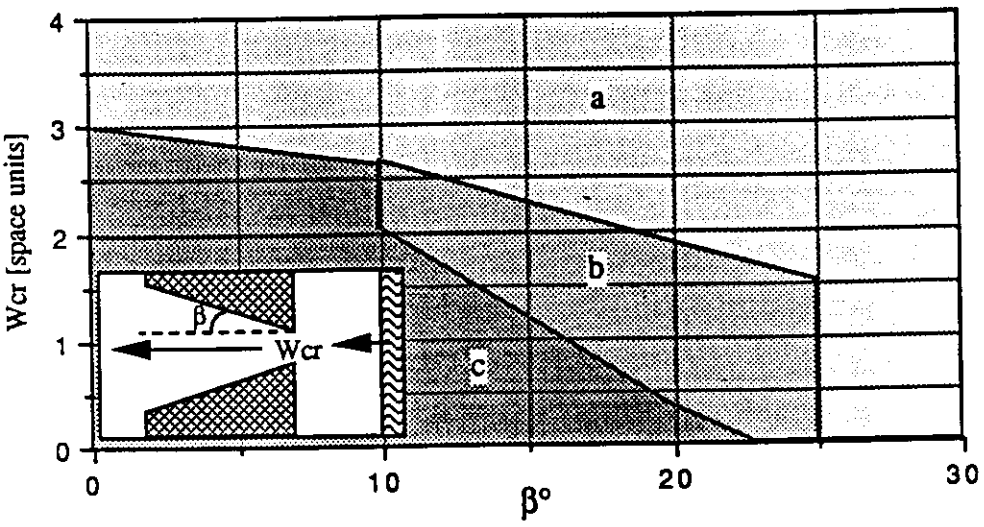

FIG. 9. The dependence of the critical width $W_n = W_{cr}$, at the narrow end of the channel, for propagation block on the taper angle β, and the excitability of the border tissue, for $G_f = 0.4$. Regions of bidirectional propagation are labeled "a", unidirectional block "b", and bidirectional block "c".

Computer simulations confirm that in these channels, as opposed to "zero flux" channels, a stationary, rectilinear wave that enters a channel has a curvilinear wave front in the channel. Fig. 10 shows computer simulation data that demonstrate that propagation velocity decreases with decreasing channel width. Data for isotropic and uniformly anisotropic ($D_y/D_x = 1/6$) tissue show that for pathways of equal width, wave propagation is slower in the isotropic tissue (Fig. 10). Tissue anisotropy also decreases the critical width of the narrow path, which allows unidirectional block. This effect of anisotropy can be explained by the decrease of current consumption in the transversal direction at the moment when the wave exits from the narrow path into the open space of survival tissue. In comparison with the case of isotropic tissue, this leads to a decrease of the wave front curvature outside the narrow pathway.

The dependence of the wave front propagation velocity on its curvature is an important characteristic of excitable tissue, which cannot be determined by direct experiments. Therefore, we used the method discussed in detail in the section entitled *Methods and Materials - Theoretical Study* see eqns. (1),(2). Eqn. (1), and (2) express the dependence of the curvature K on channel width W and gradient E component ratio. The components of the gradient E at the intersection of the wave front and channel border are found in the course of computer simulation by calculating the finite difference approximation of the partial derivatives. Fig. 11 shows the results of estimating the cur-

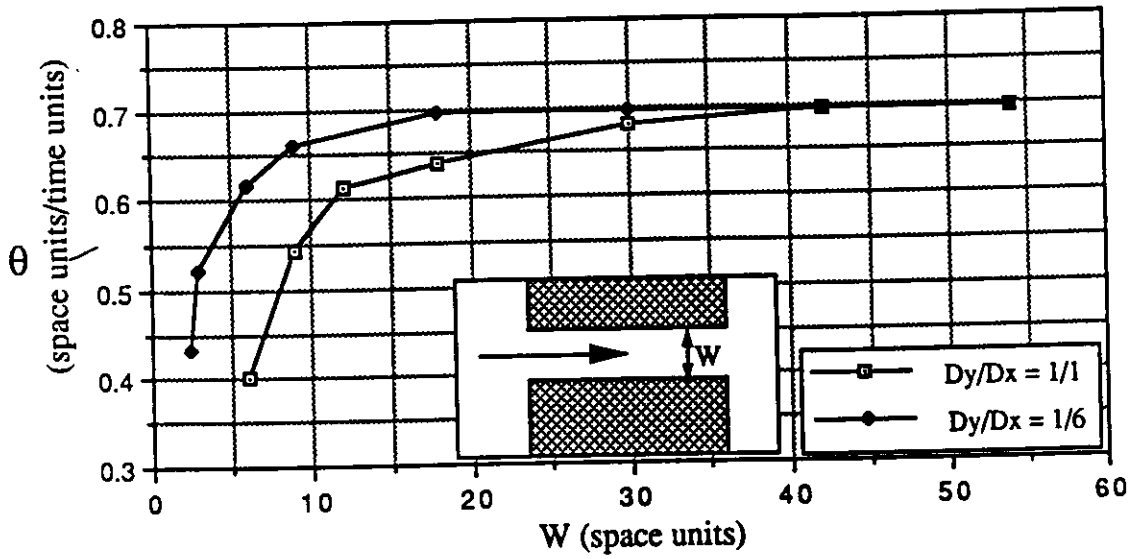

FIG. 10. The relationship of wave front velocity (θ) inside narrow paths with "large current sink" ($G_f = 0.1$) borders to the width of the channel (measured from computer simulation) is shown for both isotropic and anisotropic ($D_y/D_x = 1/6$) tissue.

vature for the same channel widths and anisotropy ratios as in Fig. 10. As expected, the curvature decreases as the channel width is enlarged. The true critical curvature (K_{cr} = maximum possible curvature) is close to the maximum K value shown in this figure. Therefore K_{cr} for anisotropic tissue is much greater than for isotropic tissue. Finally, by combining data from Fig. 10 and Fig. 11 and eliminating the parameter W, we obtained the relationship between wave front velocity and curvature (see Fig. 12). The relationship for isotropic tissue in Fig. 12 is in good agreement with data obtained for a FN model with standard parameters[25].

Reentry

The addition of another pathway, in parallel, with a width that provides $K < K_{cr}$ makes reentry possible. Initiation of reentry requires unidirectional block in the narrow path and sufficient time for this area to recover such that the returning wave front can propagate through the initial site of block. When action potential duration restitution is incorporated in the computer simulations, the recovery time becomes substantial, promoting occurrence of bidirectional block rather than unidirectional block. Delay in arrival of the returning wave front sufficient to allow reentry is promoted by anisotropy and by increasing the distance between the pathways. Indeed, Cardinal et.al. [26] have shown that the speed of propagation in the longitudinal fiber direction is 8 to 10

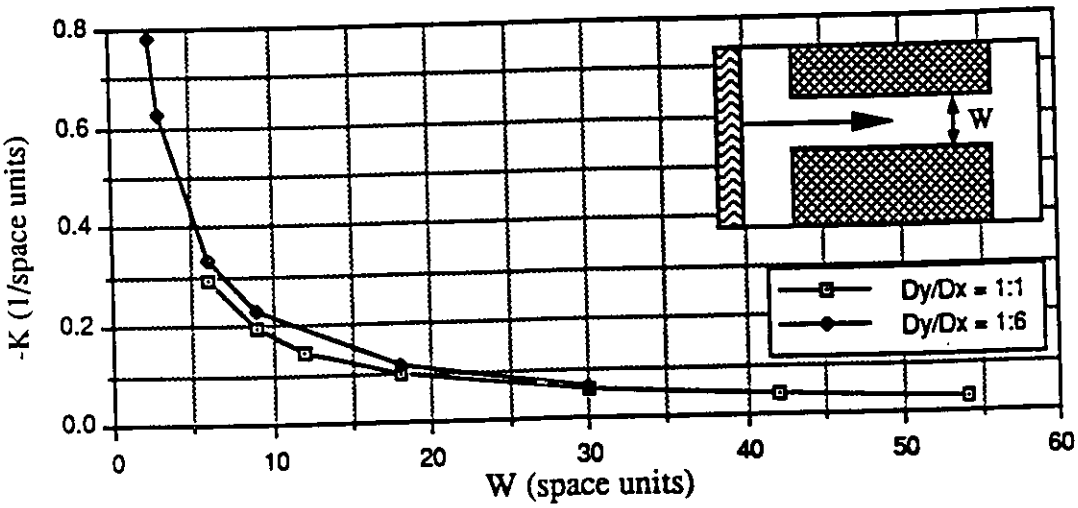

FIG. 11. The relationship of estimated wave front curvature (K) (see text, eqn. 3,4) inside narrow paths with "large current sink" ($G_f = 0.1$) borders to the width (W) of the channel is shown for computer simulations of both isotropic and anisotropic ($D_y/D_x = 1/6$) tissue.

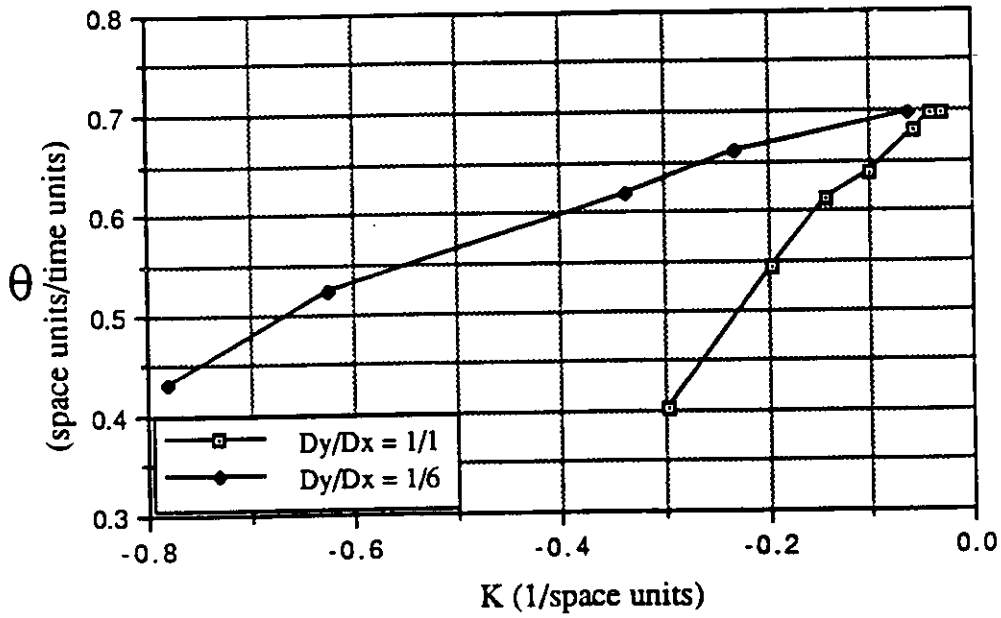

FIG. 12. The relationship of measured wave front velocity (θ) to estimated curvature (K) for modified Fitzhugh Nagumo model[21] is shown for computer simulations of both isotropic and anisotropic ($D_y/D_x = 1/6$) tissues.

times greater than in the transverse direction. Therefore, when wave propagation from one pathway to the next proceeds transverse to the long axis of the fibers, an additional time delay is introduced. This occurs when the longitudinal axis of the path and the excitable tissue inside the narrow path coincide. The latter has been observed in animal models (Janse and Wit[27]).

Narrow pathways with "zero flux" borders—

The potential reentry circuit considered consists of a single channel providing unidirectional block separated by "zero flux" tissue from a parallel wide channel. Three major cases are considered by computer simulation: 1. all viable tissue is homogeneous, isotropic, and with short time to APD restitution, 2. the same isotropic tissue but with longer time to APD restitution, and finally 3. all tissue is anisotropic with long time for APD restitution. In this way, the effect of anisotropy and APD restitution can be observed separately and jointly. Fig. 13 shows the sequence of action potential (left vertical column of pictures) and outward current (right vertical column) propagation for the first case after application a rectilinear excitation along the right side of the grid. In the absence of long APD restitution, reentry circuits of any size are easily produced.

In the second case (Fig. 14), longer APD restitution is added the conditions of the first case. Here it can be seen that the presence of residual outward current (which determines the APD restitution properties) prevents the reentrant wave from penetrating the narrow channel at the initial site of block and completing the reentry circuit. Thus the additional delay in restitution results in bidirectional block at the narrow end of the pathway.

In the final case with "zero flux" tissue bordered pathways, anisotropy (anisotropy ratio $D_x/D_y = 6/1$) is added to the conditions of the previous case. Anisotropy (Fig. 15), facilitates reentry by introducing an additional time delay for the reentrant wave to propagate in the "y" direction, allowing more time for recovery at the initial site of block. The speed of stationary wave propagation in the "y" direction is $\sqrt{6}$ times smaller than in the "x" direction. Thus, the anisotropy of the tissue facilitates reentry in the presence of narrow paths with "zero flux" borders and unidirectional block, while long time APD restitution has the opposite effect.

Narrow pathways with "large current sink" borders—

The presence of border tissue which serves as a current sink can potentially facilitate reentry by slowing conduction or inhibit reentry by promoting bidirectional block, especially when APD restitution is prolonged. The simplest case, where the tissue is isotropic and with short time for

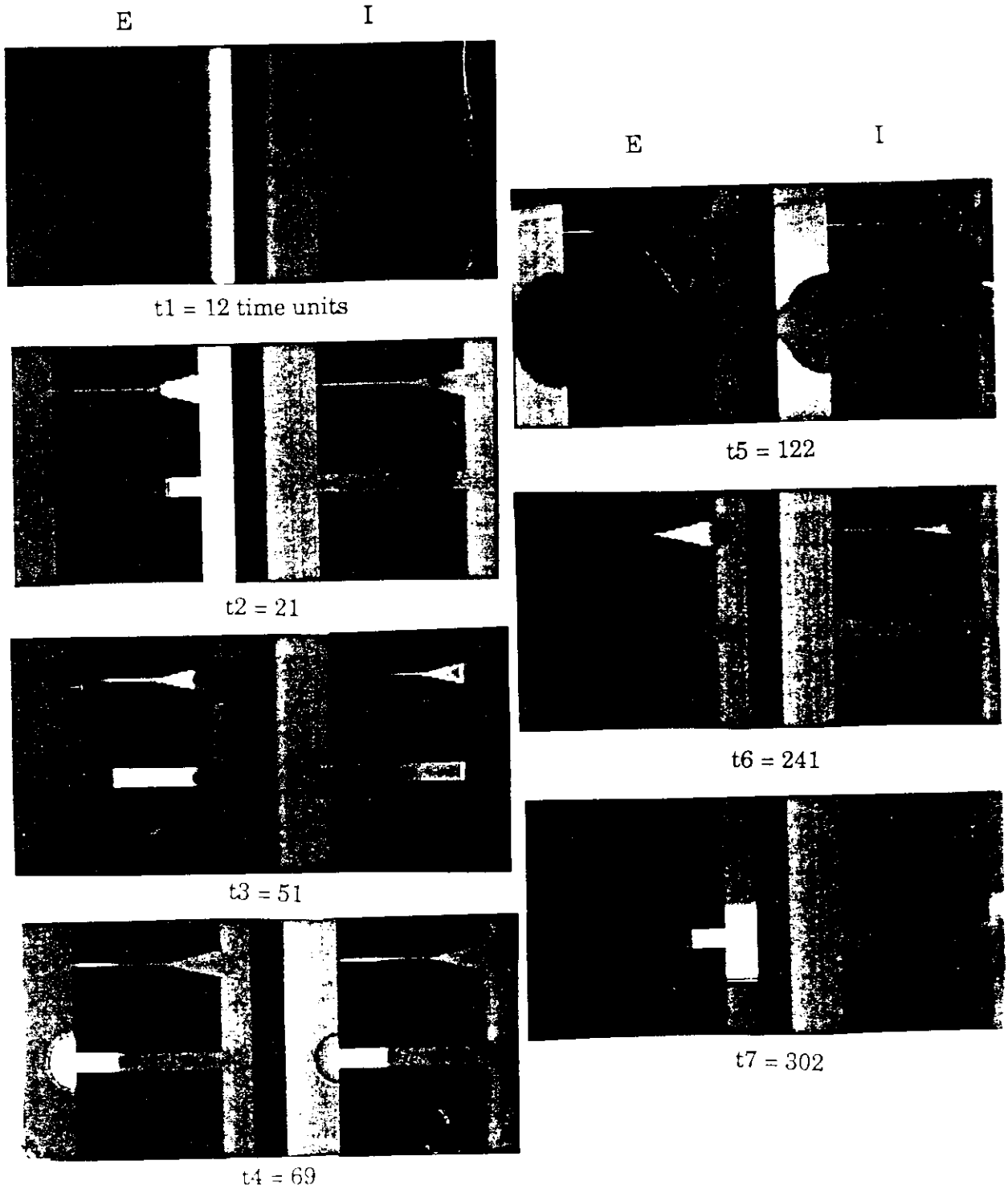

FIG. 13. Time series of reentry in homogeneous, isotropic tissue with short APD restitution properties and border tissue of the "zero flux" type. t1 – excitation begins on right edge, t2 – wave enters narrow parallel and tapered paths, t3 - continuation, t4 – excitation in tapered channel dies (block), t5 – wave reenters initial site of block, t6 – wave is unblocked as it leaves tapered path, t7 – wave reenters parallel channel

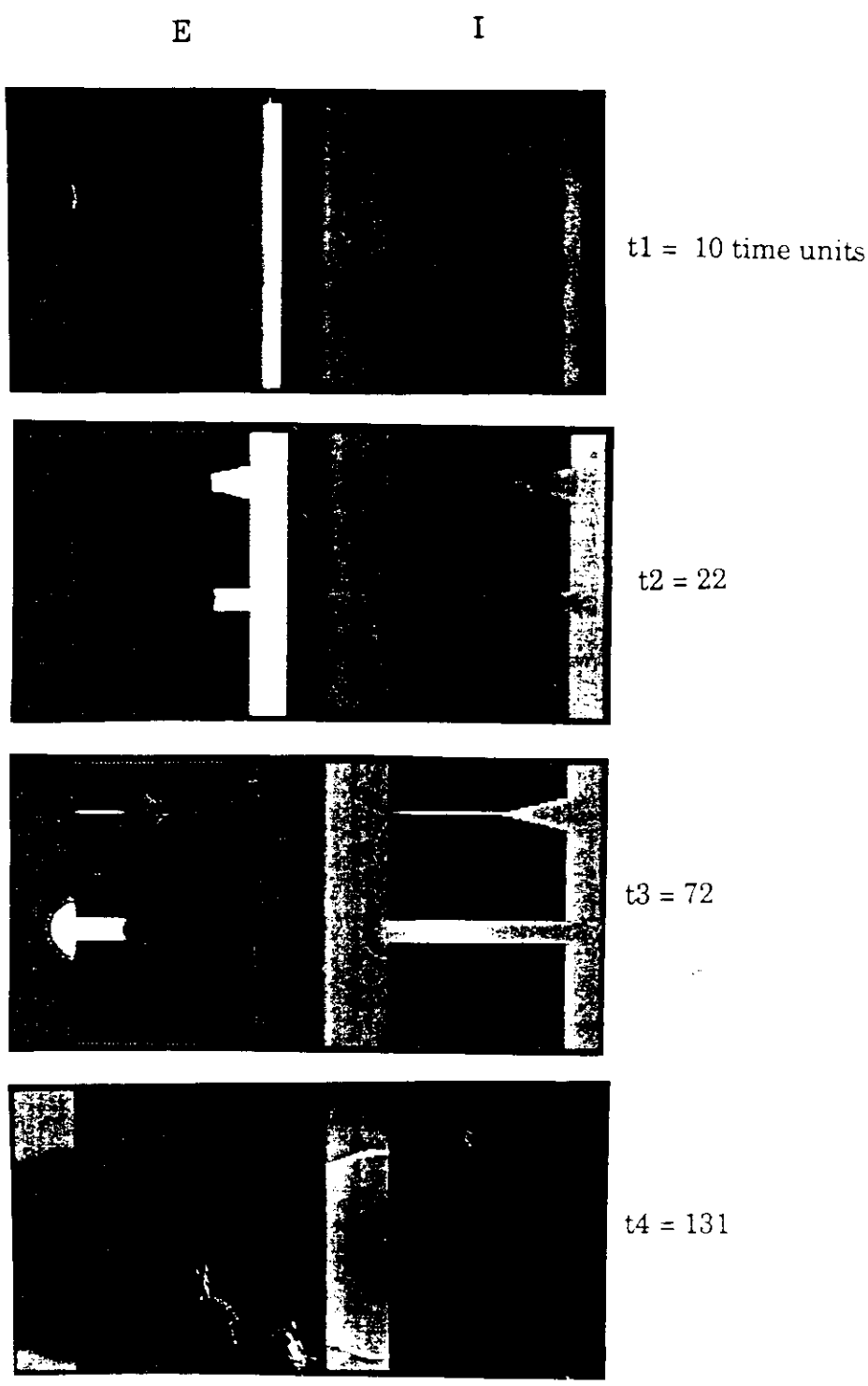

FIG. 14. Time series of reentry in homogeneous, isotropic tissue with long APD restitution properties and border tissue of the "zero flux" type. t1 – initial excitation enters from right edge, t2 – wave enters pathways, t3 – tapered channel blocks propagation, wide channel is unblocking, t4 – residual current in tapered path blocks reentering wave at initial site of block.

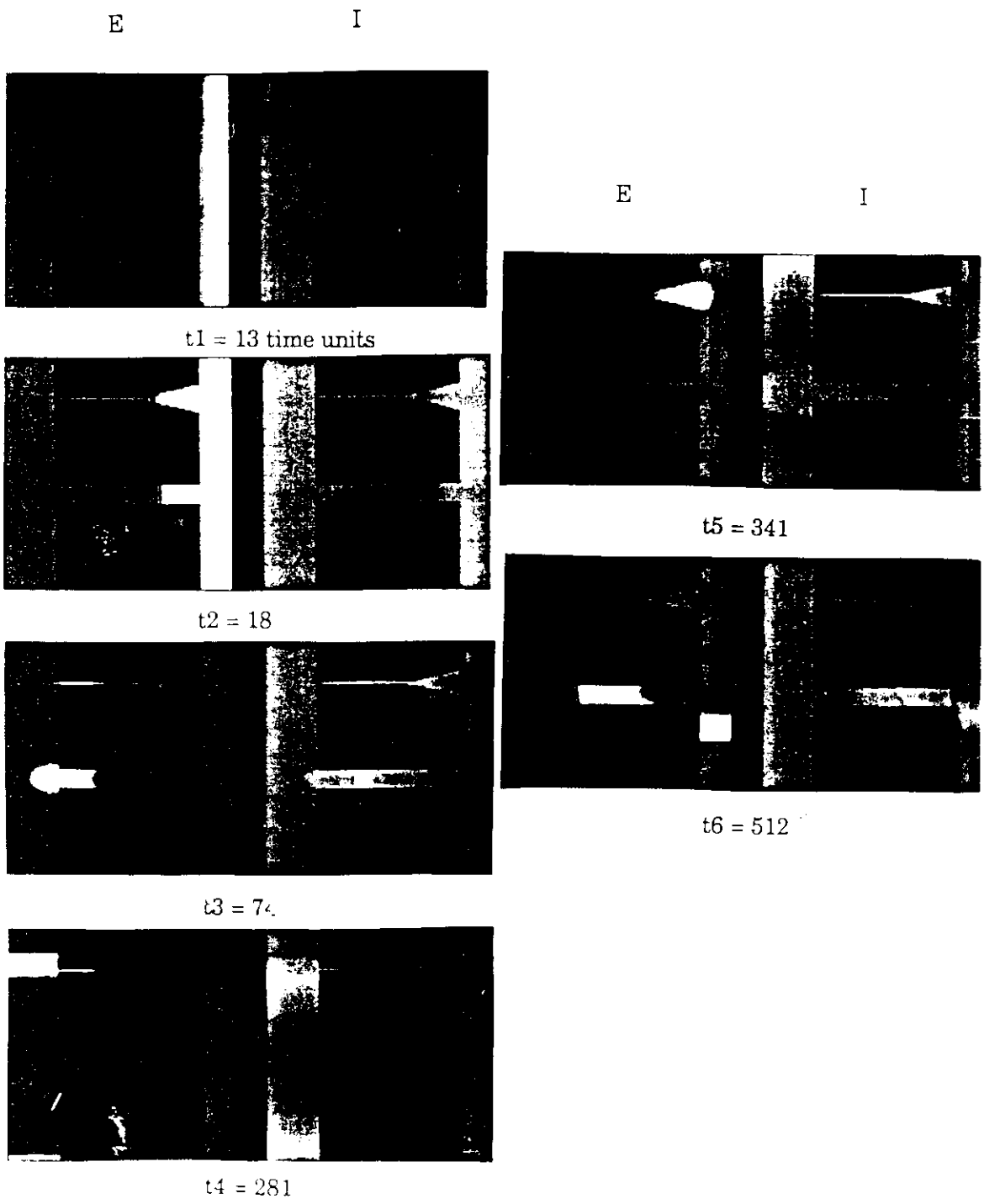

FIG. 15. Time series of reentry in uniform anisotropic tissue with long APD restitution properties ($\varepsilon_4 = 0.022$) and border tissue of the "zero flux" type. t1 – initial excitation enters from right edge, t2 – wave enters pathways, t3 – tapered channel blocks propagation, wide channel is unblocking, t4 – residual current in tapered path is too small to block reentering wave, t5 – reentry excitation continues through tapered path, t6 – wave reenters parallel wide channel

APD restitution, demonstrates that reentry can even occur with closely spaced channels (see Fig. 16).

When longer APD restitution properties are introduced into the tissue model, reentry is prevented by the residual outward current from the previous excitation of the tissue even when the spacing between the channels is increased (see Fig. 17). In this simulation anisotropy did not provide sufficient delay to avoid the effect of residual current at the initial site of block. A greater separation between paths or slowing of conduction would be required to allow reentry. Tissue anisotropy also decreases the grad$E$ component in the direction transverse to the fiber and increases it in the longitudinal direction. This increases the curvature of the wave front in the longitudinal direction, making it more difficult for the reentering wave to penetrate the narrow end of tapered channel. Therefore, for the case of narrow paths with "large current sink" border tissue, tissue anisotropy under certain conditions facilitates bidirectional block and can impede reentry.

DISCUSSION

Reentrant arrhythmias are promoted by slow conduction and unidirectional conduction block. In myocardial scars which give rise to reentrant arrhythmias the alterations in active and passive membrane properties appear to contribute to both conditions (deBakker et.al.[1], Dillon et.al.[8], Ursell et.al.[9], Spear et.al.[5]). Our analysis suggests, however, that the geometry of the surviving myocyte bands and the properties of the border tissue could also be important determinants of reentry, causing unidirectional block and slowing conduction regardless of alterations in active membrane properties or intercellular resistance within the bundles. Furthermore, the tissue anisotropy and APD restitution properties significantly influence propagation through narrow pathways, modifying the effects of geometry and potentially facilitating or inhibiting the formation of unidirectional block and reentry. Geometrical considerations may also explain the conduction properties of accessory atrioventricular pathways, consisting of narrow strands of myocytes coursing from atrium to ventricle across the atrioventricular sulcus. Conduction properties of these pathways are often markedly different in the atrioventricular compared to the ventriculoatrial directions and some pathways do not allow propagation at all in one direction yet allow rapid propagation of impulses in the opposite direction. Our findings support the notion of impedance mismatch (de la Fuenta et.al.[10], Inoue and Zipes[11]) as a cause of these discrepancies and suggest geometric configurations of conduction pathways which facilitate reentry.

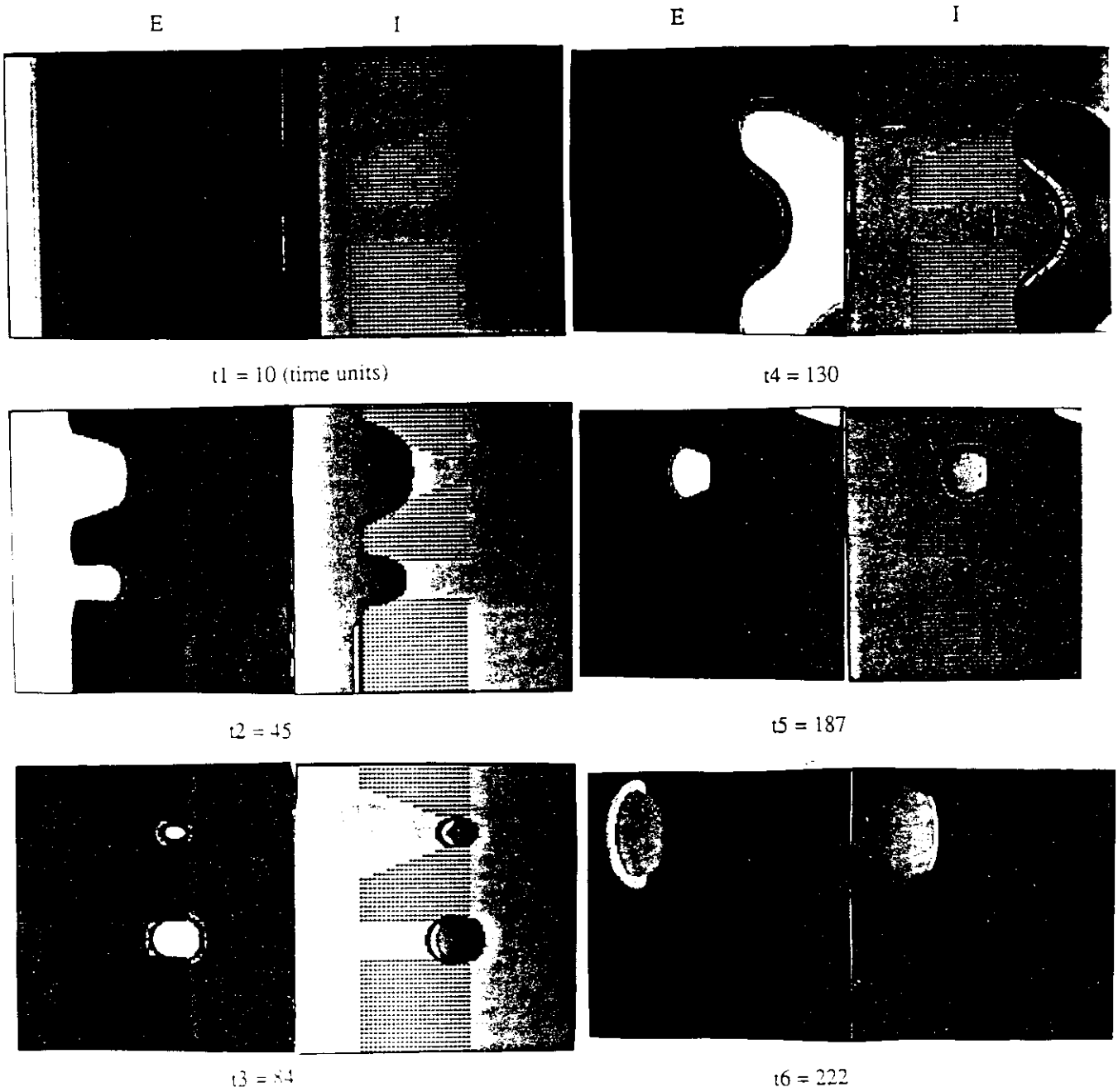

FIG. 16. Time series of reentry induced in tissue with narrow paths bordered by "large current sink" tissue. Viable tissue is homogeneous, isotropic, and with short APD restitution properties. G_f of border tissue = 0.1, path length = 30[space units], β = 20 deg, distance between center of paths = 28.5[space units]. t1 - initial excitation enters from left edge, t2 – wave enters pathways, t3 – tapered channel blocks propagation, wide channel is unblocking, t4 – tapered path does not block reentering wave, t5 - reentry excitation continues through tapered path, t6 – continuation

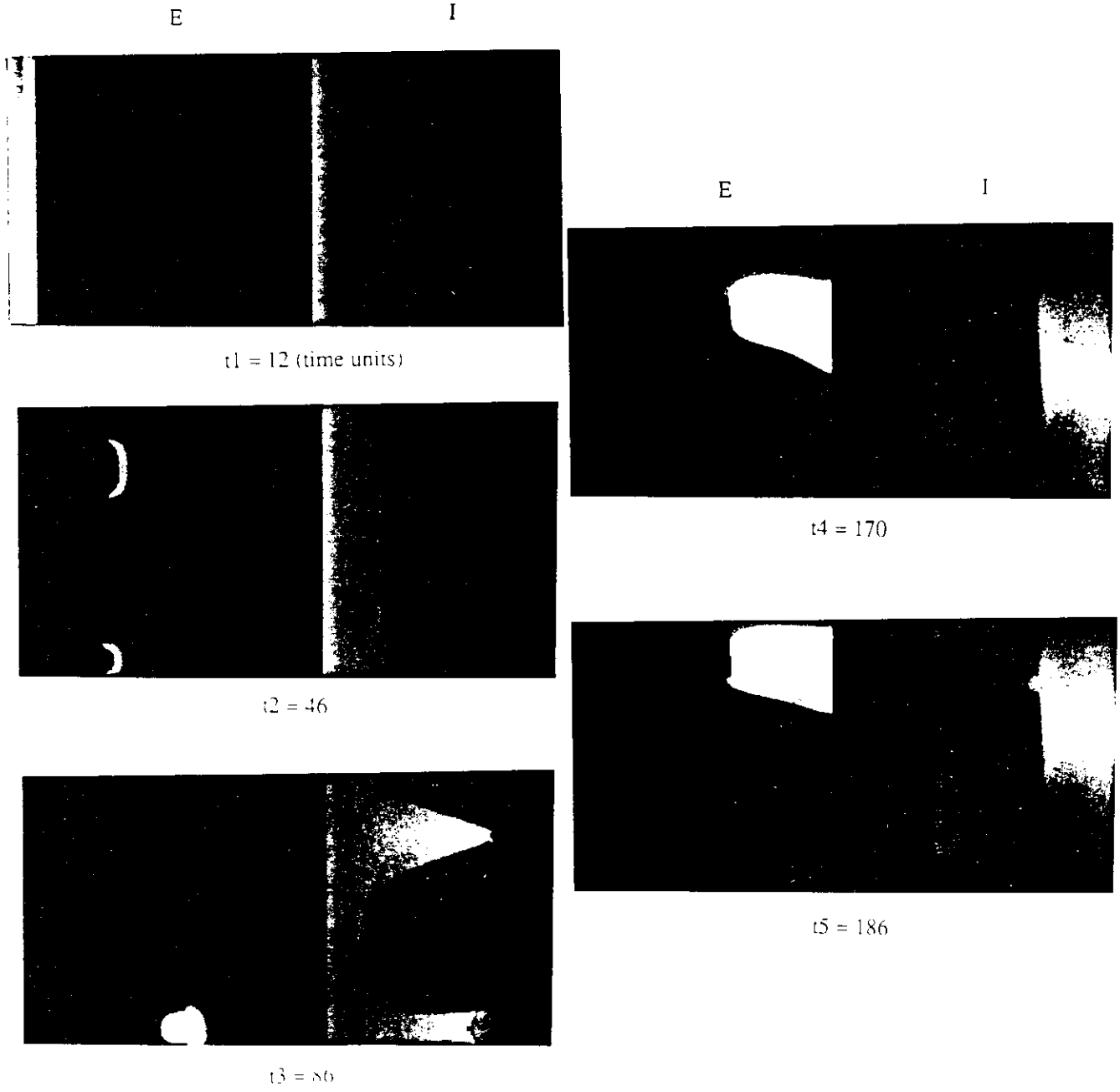

FIG. 17. Time series of failed reentry in tissue with narrow paths bordered with "large current sink" tissue. Viable tissue is homogeneous, isotropic, and has long APD restitution properties ($\varepsilon_4 = 0.022$). For border tissue $G_f = 0.1$, path length = 30[space units], $\beta = 20$ deg, distance between center of paths = 52.5[space units]. t1 - initial excitation enters from left edge, t2 – wave enters pathways, t3 – tapered channel blocks propagation, t4 – residual current blocks propagation at initial site of block, t5 - continuation

In this paper, theoretical analysis of wave propagation in excitable media is combined with computer simulations. Wave propagation through two idealized types of two dimensional narrow channels is considered. It is assumed that the border tissue can be either "zero flux", which does not serve as a current sink, or which serves as a current sink to a variable degree. The border conditions for narrow paths in infarct scars are not known. Histologic and microelectrode studies of infarct scars have shown that electrically "inert" collagen, as well as myocytes with depressed excitability and/or markedly prolonged recovery times, which could serve as an abnormal current sink, coexist with relatively normal myocytes. We also considered the influence of anisotropy of the tissue inside these narrow channels.

The theoretical results are not dependent on the type of tissue mathematical model used. These results were obtained by the combined application of the previously obtained relationship of wave front velocity (θ) to curvature (K) and the estimation of wave front grad$E$ components. Computer simulation results were obtained for the modified FitzHugh-Nagumo model [22], which permitted us to study the effect of action potential duration restitution.

The theoretical study provides the following principal results:

1. We developed an approach for estimating the wave front curvature inside narrow pathways using the geometry of the channel and the components of the grad$E$ of the wave front. These components can be obtained during computer simulations. This approach can be used for different types of mathematical models, for tissue cultures and pieces of real tissue. The similarity of the results obtained using real tissue and the mathematical model can serve as an indication of the fidelity of this model in reproducing the propagation properties.

2. Inside "zero flux" bordered pathways with finite length and openings at both ends, waves propagate with a rectilinear front only when the pathway borders are parallel. The wave front and its curvature change when passing the opening in either direction. If the pathway configuration is such that the wave front curvature reaches the critical value, conduction block occurs.

3. When the parallel borders serve as an abnormal current sink, the wave propagates or is blocked in both directions as determined by the channel width. Unidirectional block occurs only for narrow tapered paths. Under certain conditions, impulses entering from the narrow end of the tapered channel propagate, while impulses entering from the wide end die out.

4. Regardless of the properties of the narrow pathways border, the necessary condition for unidi-

rectional block is the asymmetry of pathway geometry for the waves propagated in the opposite directions.

Computer simulations show that these results are valid for the modified FN model. Simulations also illuminate the effects of tissue anisotropy and APD restitution on wave propagation in narrow paths, and on the appearance of reentry:

1. Reentry is possible for either border condition when a pathway with unidirectional block exists in parallel with at least one non-blocking channel.

2. APD restitution tends to inhibit reentry. For reentry to occur, an increased time delay for wave propagation in the reentry loop is required.

3. For narrow paths with zero flux border tissue, tissue anisotropy greatly facilitates the development of reentry (introduces natural delay) and at the same time expands the range of path width (in the direction of smaller width) for which unidirectional block and reentry are possible.

4. For narrow paths bordered by tissue serving as an abnormal current sink, tissue anisotropy can facilitate unidirectional block by increasing the time to arrival of the excitation wavefront at the initial site of block, or it can inhibit formation of unidirectional block by promoting conduction out from the narrow path.

The presented results are limited to idealized smooth two–dimensional narrow pathways with uniform anisotropy of excitable tissue. Moreover the F-N model is an oversimplification of membrane processes. Therefore, the computer simulation results have only a qualitative character. The theoretical results, which are not dependent on the limitations of a particular mathematical model, provide a means to also obtain quantitative results for some specific conditions, such as "zero flux" borders.

The study of wave propagation through nonidealized 3-dimensional bundles of excitable tissue, using more sophisticated membrane models is currently a formidable problem, not only for theoretical investigations, but also for computer simulations using the most powerful modern computers. This difficulty explains why researchers have used simplified models to investigate 3-dimensional wave propagation. For example, the computer simulation study of solitary wave propagation in 3-dimensional strands of heart muscle placed in a cylindrical saline bath was performed by Roth[28]. In that work the attention was restricted to the depolarization phase of the action potential, the

primary determinant of the speed of wave propagation. For the study of unidirectional block and reentry the repolarization phase and APD restitution are of great importance, too. Most other publications on 3-dimensional computer simulations are devoted to the study of spiral wave propagation in free 3-dimensional excitable media (see for example Winfree [29]). Another approach is to limit the computer investigation to a one dimensional model with a complex configuration using a more sophisticated membrane model[30]. In this investigation, geometric effects on unidirectional block and reentry could not be studied.

CONCLUSION

We found that in simulations of cardiac tissue having uniform membrane properties and intercellular resistance, the geometry and border conditions of narrow pathways have several important effects on impulse propagation:

1. Pathway geometry alone can lead to unidirectional block and slow conduction velocity. The necessary condition for occurrence of unidirectional block is the asymmetry of narrow pathways for waves propagated in the opposite directions.

2. Border conditions markedly alter the effects of pathway geometry.

3. Reentry can occur entirely due to the effects of pathway geometry and border conditions.

4. The concept of wave front curvature used in the present theoretical study allows us to obtain quantitative relationships between the wave front curvature inside narrow pathways, and the geometry of the pathways with the borders of "zero flux" type.

REFERENCES

[1] J.M.T. de Bakker, F.J.L. Van Capelle, M.J. Janse, A.A.M. Wilde, R. Coronel, A.E. Becker, K.P. Dingemans, N.M. Van Hemel, and R.N. Hauer. Reentry as a cause of ventricular tachycardia in patients with chronic ischemic heart disease: electrophysiologic and anatomic correlation. *Circulation*, 77:589–606, 1988.

[2] D.R. Bolick, D.B. Hackel, K.A. Reimer, and R.E. Ideker. Quantitative analysis of myocardial infarct structure in patients with ventricular tachycardia. *Circulation*, 74:1266–1279, 1986.

[3] J.J. Fenoglio, T.D. Pham, A.H. Harkes, L.N. Horowitz, M.E. Josephson, and A.L Wit. Recurrent sustained ventricular tachycardia: structure and ultrastucture of subendocardial regions in tachycardia originates. *Circulation*, 68:518–533, 1983.

[4] J.M.T. de Bakker, R. Coronel, S. Taaeron, A.A.M Wilde, T. Opthof, M.J. Janse, F.J.L. Van Capelle, A.E. Becker, and G. Jambroes. Ventricular tachycardia in the infarcted, langendorff-perfused human heart: role of the arrangement of surviving cardiac fibers. *J Am Coll Cardiol*, 15:1594–1607, 1990.

[5] J.F. Spear, L.N. Horowitz, A.B. Hodess, H. Mac Vaugh, and E.N. Moore. Cellular electrophysiology of human myocardial infarction: abnormalities of cellular activation. *Circulation*, 59:247–256, 1979.

[6] P.I. Gardner, P.C. Ursell, J.J. Fenoglio, and A.L. Wit. Electrophysiologic and anatomic basis for fractionated electrograms recorded from healed myocardial infarcts. *Circulation*, 72:596–611, 1985.

[7] A.R. Denniss, D.A. Richards, J.A. Waywood, T. Yung, C.A. Kam, D.L. Ross, and J.B. Uther. Electrophysiological and anatomic differences between canine hearts with inducible ventricular tachycardia and fibrillation associated with chronic myocardial infarction. *Circ Research*, 64:155–166, 1989.

[8] S.M. Dillon, M.A. Allessie, P.C. Ursell, and A.L. Wit. Influences of anisotropic tissue structure on reentrant circuits in the epicardial border zone of subacute canine infarcts. *Circ. Research*, 63:182–206, 1988.

[9] P.C. Ursell, P.I. Gardner, A. Albala, J.J. Fenoglio, and A.L. Wit. Structural and electrophysiological changes in the epicardial border zone of canine myocardial infarcts during infarct healing. *Circ. Research*, 56:436–451, 1985.

[10] D. de la Fuente, B. Sasyniuk, and G.K. Moe. Conduction through a narrow isthmus in isolated canine atrial tissue, a model of wpw syndrome. *Circulation*, 44:803–809, 1971.

[11] H. Inoue and D.P. Zipes. Conduction over an isthmus of atrial myocardium in vivo: a possible model of wolff-parkinson-white syndrome. *Circulation*, 76, 1987.

[12] C. Mendez, W.J. Mueller, and X. Urguiaga. Propagation of impulses across the purkinje fiber-muscle junctions in dog heart. *Circ. Research*, 26:135–150, 1970.

[13] V.S. Zykov. Analytic estimate of the dependence of excitation wave velocity in a two dimensional excitable medium on the curvature of its front. *Biofizika*, 25(5), 1980.

[14] J.J. Tyson and J.P. Keener. Singular perturbation theory of traveling waves in excitable media. *Physica D*, 32:327–361, 1988.

[15] B.Y. Kogan, W.J. Karplus, and B.S. Billett. Excitation wave propagation along narrow pathways, unidirectional block and reentry (theoretical study). Technical Report 910053, Computer Science Department, UCLA, July 1991.

[16] A.L. Wit, S.M. Dillon, J. Coromiles, A.E. Soltman, and B. Waldecker. Anisotropic reentry in the epicardial border zone of myocardial infarcts. In J. Jalife, editor, *Mathematical Approach to Cardiac Arrythmias: Annals of New York Academy of Sciences*, volume 591, pages 62–74. The New York Academy of Sciences, 1990.

[17] M.S. Spach, P.C. Dolber, and J.F. Hudlage. Properties of discontinuous anisotropic propagation at a microscopic level. In J. Jalife, editor, *Mathematical Approach to Cardiac Arrythmias: Annals of New York Academy of Sciences*, volume 591, pages 62–74. The New York Academy of Sciences, 1990.

[18] Y. Rudy and W. Quan. A model study of the effect of discrete cellular structure on electrical propagation in cardiac tissue. *Circ. Res.*, 61(6), 1987.

[19] R.F. Gilmour, J.J. Heger, E.N. Prystowsky, and D.P. Zipes. Cellular electrophysiology abnormailies of diseased human ventricular myocardium. *Am J Cardiology*, 51:137–144, 1983.

[20] R.J. Myerburg, K Epstein, M.S. Gaide, S.S. Wong, A. Castellanos, H. Gelband, J.S. Cameron, and A.L. Basset. Cellular electrophysiology in acute and healed experimental myocardial infarction. *Ann New York Acad Sci*, pages 90–113, 1982.

[21] B.Y. Kogan, W.J. Karplus, and A.T. Pang. Simulation of nonlinear distributed parameter systems on the connection machine. *Simulation*, 55:271–280, 1990.

[22] B.Y. Kogan, W.J. Karplus, B.S. Billett, A.T. Pang, H.S. Karagueuzian, and Khan S.S. The simplified fitzhugh - nagumo model with action potential duration restitution: Effects on 2-d wave propagation. *Physica D*, 50:327–340, 1991.

[23] A.A. Petrov. Hybrid method of solving partial differential equations. *Avtom. Telemeka.*, 3, 1975.

[24] A.T. Pang. *On Simulating and Visualizing Nonlinear Distributed Parameter Systems Using Massively Parallel Computers.* PhD thesis, UCLA, 1990.

[25] V.S. Zykov. *Simulation of Wave Processes in Excitable Media.* Manchester University Press, 1987.

[26] R. Cardinal, M. Vermulen, M. Shenasa, F. Roberge, P. Page, and F. Helie. Anisotropic conduction and functional dissociation of ischemic tissue during reentrant ventricular tachycardia in canine myocardial infarction. *Circulation*, 77:1162–1176, 1988.

[27] M.J. Janse and A.L. Wit. Electrophysiological mechanisms of ventricular arrythmias resulting from myocardial ischemia and infarction. *Physiol. Rev.*, 69:1049–1169, 1989.

[28] B.J Roth. Action potential propagation in a thick strand of cardiac muscle. *Circul. Res.*, 68:162–173, 1991.

[29] A.T. Winfree. The electrical thresholds of ventricular myocardium. *Journal of Cardiovascular Electrophysiology*, 1:393–410, 1990.

[30] C. Delgado, B. Steinhaus, M. Delmar, D.R. Chialvo, and J. Jalife. Directional differenced in excitability and margin of safety for propagation in sheep ventricular epicardial muscle. *Circul. Res.*, 67:97–110, 1990.